

DESY 13-127  
Edinburgh 2013/18  
Liverpool LTH 983  
September 2013

## The SU(3) Beta Function from Numerical Stochastic Perturbation Theory

R. Horsley<sup>a</sup>, H. Perlt<sup>b,c</sup>, P.E.L. Rakow<sup>d</sup>, G. Schierholz<sup>e</sup> and A. Schiller<sup>b</sup>

<sup>a</sup> School of Physics and Astronomy,  
University of Edinburgh,  
Edinburgh EH9 3JZ, United Kingdom

<sup>b</sup> Institut für Theoretische Physik,  
Universität Leipzig,  
04103 Leipzig, Germany

<sup>c</sup> Helmholtz Institut für Strahlen- und Kernphysik,  
Universität Bonn,  
53115 Bonn, Germany

<sup>d</sup> Theoretical Physics Division,  
Department of Mathematical Sciences,  
University of Liverpool,  
Liverpool L69 3BX, United Kingdom

<sup>e</sup> Deutsches Elektronen-Synchrotron DESY,  
22603 Hamburg, Germany

### Abstract

The SU(3) beta function is derived from Wilson loops computed to 20<sup>th</sup> order in numerical stochastic perturbation theory. An attempt is made to include massless fermions, whose contribution is known analytically to 4<sup>th</sup> order. The question whether the theory admits an infrared stable fixed point is addressed.

The evolution of the running coupling  $g^2(\mu)$  of nonabelian gauge theories as a function of the Euclidean momentum scale  $\mu$  is of fundamental interest. It is encoded in the Callan-Symanzik  $\beta$  function. Of particular interest is the evolution of  $g^2(\mu)$  at small momenta, which is determined by the behavior of the  $\beta$  function at large  $g^2$ . Three possibilities come to mind. In the pure gauge theory the most plausible, and internally consistent, scenario is that  $\mu$  cannot be taken lower than a certain value,  $\mu_0 \leq \mu$ , where  $\mu_0$  is the ‘mass gap’ of the theory.<sup>1</sup> In the theory with dynamical massless fermions there is no mass gap, and nothing stops  $\mu$  from being taken to zero. Whether the  $\beta$  function exhibits an infrared fixed point and  $g^2(\mu)$  freezes at small scales  $\mu$ , giving rise to a conformal window, is an open question though. The third scenario is that the  $\beta$  function has a pole at some finite value of  $g^2$ , like that of the supersymmetric Yang-Mills theory [1]. Actually, this is a special case of the first scenario. It will divide the theory into two phases, one being asymptotically free and another being strongly coupled in the infrared, with  $g^2(\mu)$  flowing to a point  $g^{*2}$ , both from the small and large  $g^2$  domain. In this work we shall seek an ‘all-order’ perturbative solution to the SU(3)  $\beta$  function.

We start from rectangular  $L \times T$  Wilson loops  $W(L, T)$  and the corresponding Creutz ratios  $R(L, T)$ ,

$$R(L, T) = \frac{W(L, T) W(L-1, T-1)}{W(L, T-1) W(L-1, T)}. \quad (1)$$

For  $T \gg L$  the Wilson loops can be written

$$W(L, T) = C \exp \{-E(L) T\}, \quad E(L) = -\tilde{C}_F \frac{g_V^2(L)}{L} + \sigma L - \frac{\pi}{12L}, \quad (2)$$

where  $\tilde{C}_F = C_F/4\pi = 1/3\pi$ . The string tension  $\sigma$  and the contribution  $-\pi/12L$  from fluctuations of the bosonic string [2] are of nonperturbative origin and will be discarded in the following. The factor  $C$ , with  $\ln C \propto (L + T)$ , drops out in the Creutz ratio. This leaves us with

$$\ln R(L, T) = \tilde{C}_F \left[ \frac{g_V^2(L)}{L} - \frac{g_V^2(L-1)}{L-1} \right]. \quad (3)$$

If we now expand  $g_V^2(L)$  and  $g_V^2(L-1)$  around  $L = \bar{L} \equiv \sqrt{L(L-1)}$ ,  $g_V^2(L) = g_V^2(\bar{L}) + g_V^{2'}(\bar{L})(L - \bar{L}) + \dots$ , we find

$$\ln R(L, T) = \tilde{C}_F \left[ -\frac{g_V^2(\bar{L})}{\bar{L}^2} + \frac{g_V^{2'}(\bar{L})}{\bar{L}} \right] \equiv -\tilde{C}_F \frac{g_{qq}^2(\bar{L})}{\bar{L}^2} = -F(\bar{L}), \quad (4)$$

up to a systematic error  $\simeq -\tilde{C}_F g_V^{2'''}(\bar{L})/24\bar{L}$  arising from the truncation of the Taylor series, where  $F(L)$  is the force and  $g_{qq}^2(L)$  the coupling in the  $qq$  or force scheme. The corresponding  $\beta$  function,  $\beta_{qq}(g_{qq}(L))$ , is given by

$$\frac{1}{2 g_{qq}(L)} \frac{\partial g_{qq}^2(L)}{\partial \ln L} = -\beta_{qq}(g_{qq}(L)), \quad (5)$$

---

<sup>1</sup>This might be the dynamically generated mass of the gluon.

from which the running coupling  $g_{qq}^2(\mu)$ , with  $\mu = 1/L$ , may be obtained by solving

$$\frac{\mu}{\Lambda_{qq}} = (\beta_0 g_{qq}^2(\mu))^{\frac{\beta_1}{2\beta_0}} \exp \left\{ \frac{1}{2\beta_0 g_{qq}^2(\mu)} + \int_0^{g_{qq}^2(\mu)} dg \left( \frac{1}{\beta_{qq}(g)} + \frac{1}{\beta_0 g^3} - \frac{\beta_1}{\beta_0^2 g} \right) \right\}. \quad (6)$$

Perturbatively, the  $\beta$  function

$$\beta_{qq}(g) = -g^3 (\beta_0 + \beta_1 g^2 + \beta_2^{qq} g^4 + \dots) \quad (7)$$

is known to four loops [3]. The first two coefficients are universal,  $\beta_0 = 11/(4\pi)^2$ ,  $\beta_1 = 102/(4\pi)^4$ , while the remainder are scheme dependent.

In [4] we have computed rectangular Wilson loops  $W(L, T)$  on the  $12^4$  lattice for  $L, T = 1, \dots, 6$  to  $N = 20$  loops in the bare coupling  $g_0^2$ , using numerical stochastic perturbation theory [5] and the Wilson gauge action. We did not encounter any renormalon singularities. The perturbative series of the smaller Wilson loops were estimated to converge for  $g_0^2 \leq 1.04$ . Knowing the Wilson loops, we can compute the Creutz ratios. The latter can be written

$$R(L, T) = 1 + \sum_{n=1}^N r_n(L, T) g_0^{2n}, \quad (8)$$

from which we obtain the running coupling

$$g_{qq}^2(\bar{L}) = \frac{1}{r_1(L, T)} \ln R(L, T) = g_0^2 + \sum_{n=2}^N c_n(L, T) g_0^{2n}. \quad (9)$$

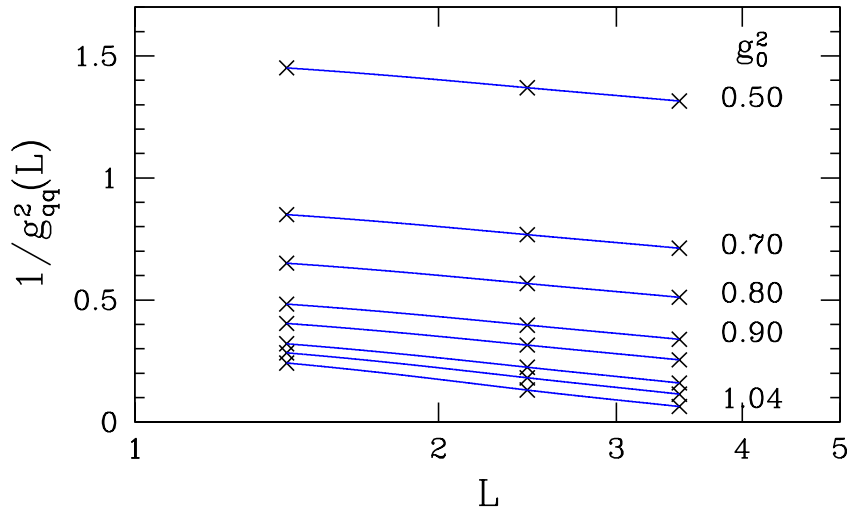


Figure 1: A plot of the coupling  $g_{qq}(L)$  as a function of  $\ln L$ . The crosses ( $\times$ ) show the lattice results for bare couplings  $g_0^2 = 0.5, \dots, 0.9, 0.95, 1.0, 1.02, 1.04$ , from top to bottom. The curves show a second-order Lagrange interpolation of the lattice data.

We consider Wilson loops of size  $T = 5$  and  $L = 2, 3$  and  $4$ . This leaves us with the Creutz ratios  $R(2, 5)$ ,  $R(3, 5)$  and  $R(4, 5)$ , from which we obtain  $g_{qq}^2(\bar{L})$  at  $\bar{L} = \sqrt{2}$ ,  $\sqrt{6}$  and  $\sqrt{12}$ . In first (one-loop) approximation  $g_{qq}^{-2}(L)$  is a linear function of  $\ln L$ . In Fig. 1 we plot  $g_{qq}^{-2}(L)$  against  $\ln L$  for various values of  $g_0^2$ . At  $g_0^2 = 1.04$  we find  $g_{qq}^2(\sqrt{12}) \approx 16$ , which allows us to probe rather large values of the running coupling. We employ a second-order Lagrange polynomial in  $\ln L$  for interpolation of  $g_{qq}^{-2}(L)$ . The result is shown in Fig. 1 as well. The  $\beta$  function is then obtained from

$$\frac{1}{2} \frac{\partial g_{qq}^{-2}(L)}{\partial \ln L} = \bar{\beta}_{qq}(g_{qq}(L)), \quad (10)$$

where  $\bar{\beta}(g) = g^{-3} \beta(g)$ .

The first two coefficients of the  $\beta$  function can directly be read off from the perturbative expansion of  $\bar{\beta}_{qq}$  in powers of  $g_0^2$ ,  $\bar{\beta}_{qq} = -(\beta_0 + \beta_1 g_0^2 + \dots)$ , with  $\beta_0 = (1/2) \partial c_2 / \partial \ln L$  and  $\beta_1 = (1/2) \partial (c_3 - c_2^2) / \partial \ln L$ . The renormalization group predicts that both  $c_2$  and  $(c_3 - c_2^2)$  are linear functions of  $\ln L$ . The first coefficient turns out to be  $\beta_0 = 11.8/(4\pi)^2$ , independent of  $L$ , as expected. The second coefficient,  $\beta_1$ , is somewhat special. It is a small difference of large numbers, with the condition that the quadratic terms  $\propto \ln^2 L$  in  $c_3$  and  $c_2^2$  cancel. The cancellation is not perfect, which makes  $\beta_1$  depend on  $L$ . At  $L = \sqrt{6}$ , the midpoint, we find  $\beta_1 = 115/(4\pi)^4$ . At this point (10) coincides with the textbook central derivative. Alternatively, we may fit a linear curve to  $(c_3 - c_2^2)$ . A weighted fit gives  $\beta_1 = 141(90)/(4\pi)^4$ , with a correlation coefficient of  $r = -0.99$ ,

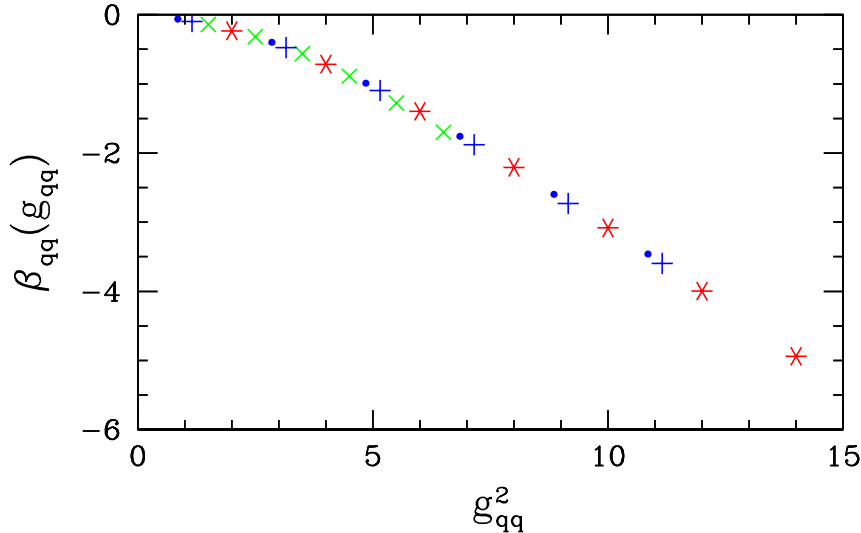


Figure 2: The full  $\beta$  function for  $N = 20$  and  $L = \sqrt{6}$  ( $\times$ ),  $L = \sqrt{9}$  ( $+$ ) and  $L = \sqrt{12}$  ( $\ast$ ), together with the  $\beta$  function truncated at  $N = 15$  for  $L = \sqrt{9}$  ( $\bullet$ ). The bare coupling has been limited to  $g_0^2 \leq 1.04$ .

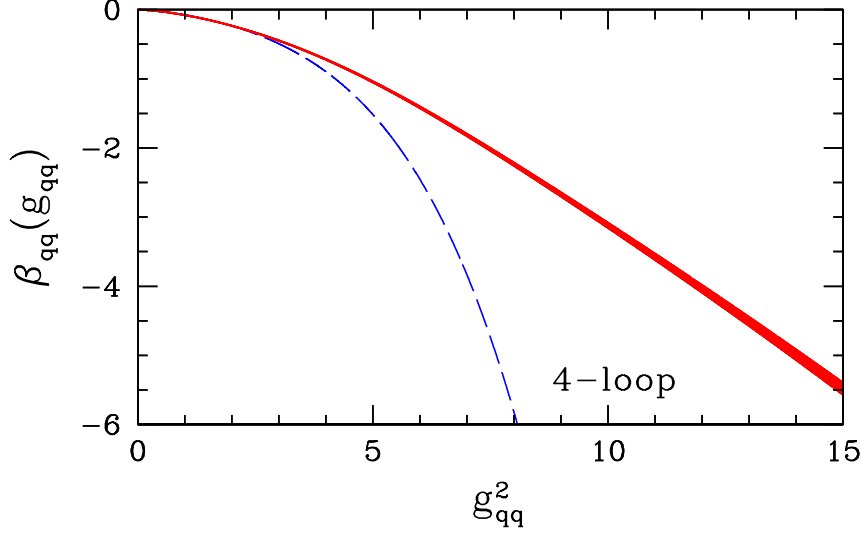


Figure 3: The  $\beta$  function  $\beta_{qq}$  against the coupling  $g_{qq}^2$ . The solid band shows the lattice result, including the error. The dashed curve shows the analytic four-loop result.

indicating that the (two) fit parameters are strongly correlated.<sup>2</sup> As an estimator for the weight factor we have used the systematic error of  $g_{qq}^2(\bar{L})$ , which is estimated to be  $\propto 1/\bar{L}^2$  (mod logs, see (4) *et seq.*). The higher coefficients of  $\beta_{qq}$  are no longer linear functions of  $\ln L$ .

We now turn to the full  $\beta$  function. Sources of error are discretization effects and malconvergence of the perturbative series. To test for possible discretization errors, we compare  $\beta_{qq}(g_{qq})$  for  $L = \sqrt{6}$ ,  $\sqrt{9}$  and  $\sqrt{12}$  in Fig. 2. We do not see any significant dependence on  $L$ . To test whether the perturbative series has converged, we compare  $\beta_{qq}(g_{qq})$  for  $N = 20$  and  $N = 15$ . We see no difference either. We start to see a difference only when the series is truncated at  $N \approx 10$ . This indicates that the  $\beta$  function is not sensitive to very large ( $N \gtrsim 10$ ) loops, as long as we keep the bare coupling below  $g_0^2 \approx 1.04$ .

In Fig. 3 we plot our final result for the  $\beta$  function. The error band shows the variance of  $\beta_{qq}(g_{qq})$  as  $L$  is varied between  $L = \sqrt{6}$  and  $\sqrt{12}$ .<sup>3</sup> We compare our result with the analytic four-loop formula [3]. The difference grows rapidly with  $g_{qq}^2$ . At  $g_{qq}^2 = 6.3$  ( $\alpha_{qq} = 0.5$ ) the full  $\beta$  function is about half the size of the four-loop analytic result, and at  $g_{qq}^2 = 8.2$  ( $\alpha_{qq} = 0.65$ ) it is one third the size only. For want of an analytic expression, the lattice  $\beta$  function can be very well described by the [3, 3] Padé approximant

$$\beta_{qq}(g_{qq}) = -g_{qq}^3 \left( \frac{\beta_0 + a_1 g_{qq}^2 + a_2 g_{qq}^4 + a_3 g_{qq}^6}{1 + b_1 g_{qq}^2 + b_2 g_{qq}^4 + b_3 g_{qq}^6} \right). \quad (11)$$

<sup>2</sup>We have not attempted a correlated fit, which we do not consider very meaningful in this case.

<sup>3</sup>This is based on a Padé fit of the form (11) to the lattice data with  $g_0^2 \leq 1.04$ .

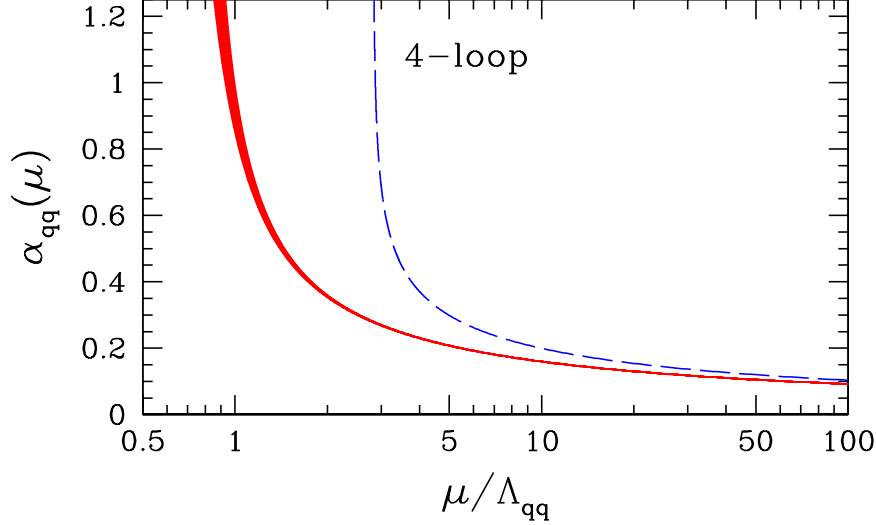


Figure 4: The running coupling  $\alpha_{qq}(\mu)$  as a function of  $\mu/\Lambda_{qq}$ . The solid band shows the lattice result, including the error. The dashed curve shows the analytic four-loop result.

It allows  $\beta_{qq}(g_{qq})$  to evolve asymptotically with any power of  $g_{qq}$  from  $-3$  to  $+9$  and have several zeroes and poles. Using MINUIT, we fit (11) to the lattice  $\beta$  function at  $L = \sqrt{9}$  with  $\beta_0 (= 0.074724)$  and  $a_1 - \beta_0 b_1 = \beta_1 (= 0.004612)$  fixed at the one- and two-loop values. The fit gives  $a_2 = -0.008910$ ,  $a_3 = 0.001550$ ,  $b_1 = 1.3008$ ,  $b_2 = -0.1605$ ,  $b_3 = 0.0200$ . The difference between the lattice result and the fit is practically invisible. We find that (11) has no poles and no zeroes on the positive real axis, in contrast to Padé fits to the four-loop  $\beta$  function [6]. Instead, (11) has one pole on the negative real axis and two poles deep in the complex. The same applies to the zeroes of the  $\beta$  function. Solving (6) for  $g_{qq}^2(\mu)$ , we obtain the running coupling  $\alpha_{qq}(\mu) = g_{qq}^2(\mu)/4\pi$  shown in Fig. 4. The interesting result is that  $\alpha_{qq}(\mu)$  hits a wall at  $\mu/\Lambda_{qq} \approx 0.7$ , indicating that  $\mu$  cannot be taken lower than  $\approx 0.7\Lambda_{qq}$ . The lambda parameter in the force scheme is  $\Lambda_{qq} = 1.048 \Lambda_{\overline{MS}}$ . Thus,  $\alpha_{qq}$  and  $\alpha_{\overline{MS}}$  lie close together. From [7] we obtain  $\Lambda_{qq} = 254(2)$  MeV, taking  $r_0 = 0.5$  fm to set the scale. It is tempting now to include fermions. The contribution of massless fermions is known to four loops [3]. Adding together the gluonic and fermionic contribution, we arrive at the  $\beta$  function for  $N_f$  quark flavors

$$\begin{aligned} \beta_{qq}^{N_f}(g_{qq}) = & \beta_{qq}(g_{qq}) - g_{qq}^3 \left[ \beta_0^{N_f} + \beta_1^{N_f} g_{qq}^2 + \beta_2^{qq, N_f} g_{qq}^4 \right. \\ & \left. + \beta_3^{qq, N_f} g_{qq}^6 + \beta_{3,l}^{qq, N_f} g_{qq}^6 \ln(3g_{qq}^2/8\pi) \right]. \end{aligned} \quad (12)$$

We are interested in the low-energy behavior of  $\alpha_{qq}(\mu)$ . This is governed by the  $u$  and  $d$  quarks, which can be assumed to be massless. We thus are led to consider the case  $N_f = 2$ . In view of successful predictions of higher-order contributions in the past [8], we fit a  $[3, 3]$  Padé approximant

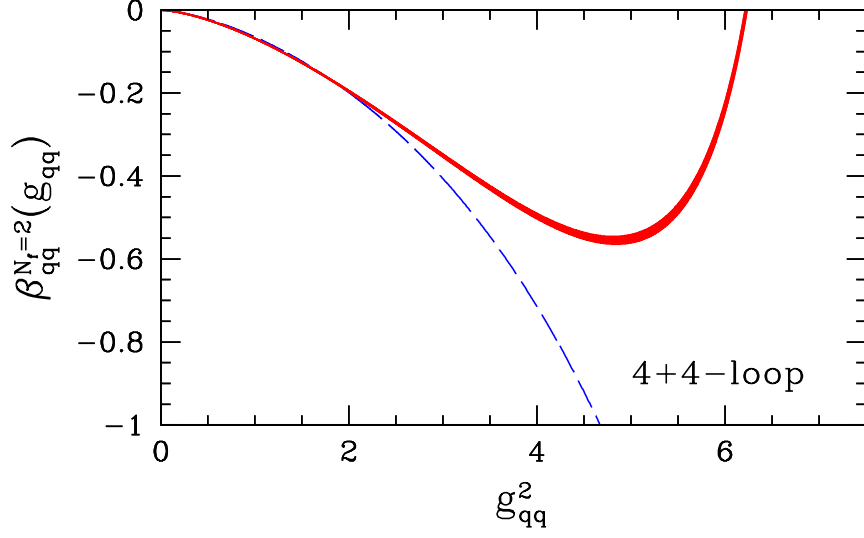


Figure 5: The  $\beta$  function  $\beta_{qq}^{N_f=2}$  against the coupling  $g_{qq}^2$ . The solid band shows the result of the Padé fit, including the error of the pure gauge part. The dashed curve shows the analytic 4 + 4-loop result.

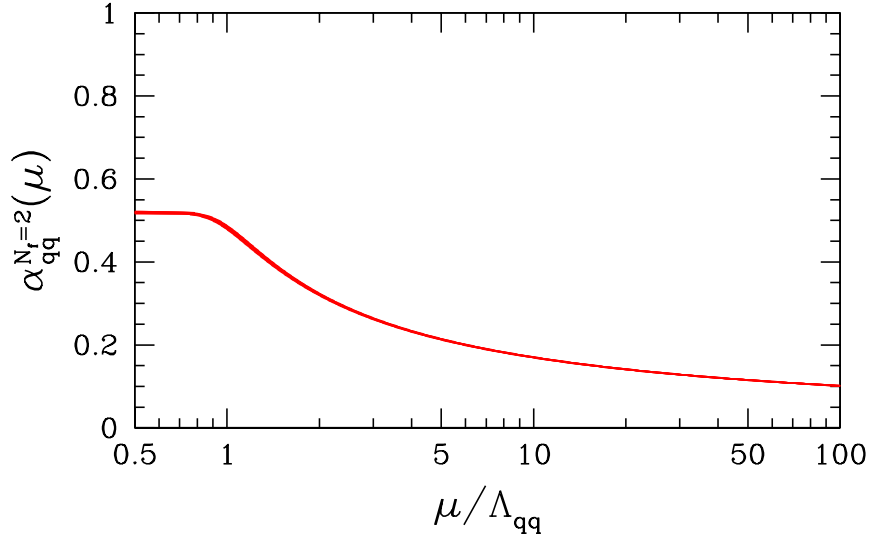


Figure 6: The running coupling  $\alpha_{qq}^{N_f=2}(\mu)$  as a function of  $\mu/\Lambda_{qq}$ , including the error.

to (12). The result of the fit is

$$\beta_{qq}^{N_f=2}(g_{qq}) = -g_{qq}^3 \left( \frac{0.066281 + 0.090111 g_{qq}^2 - 0.010112 g_{qq}^4 - 0.000857 g_{qq}^6}{1 + 1.3053 g_{qq}^2 - 0.1711 g_{qq}^4 - 0.0041 g_{qq}^6} - 0.000044 g_{qq}^6 \ln g_{qq}^2 \right), \quad (13)$$

where we have kept the logarithmic contribution separate. This is justified, as the latter contributes only a few percent in the region that is of interest to us. The  $\beta$  function (13) is shown in Fig. 5. It has a zero at  $g_{qq}^2 = 6.3$  followed by a pole at  $g_{qq}^2 = 7.3$ . The other two poles lie on the negative real axis. The coefficient  $a_1$  (in the notation of (11)) underwent the biggest change, while  $b_1$  has practically not changed at all, and the subleading negative coefficients  $a_2$  and  $b_2$  have changed by 15% or less, as compared to (11). For the  $[3, 3]$  Padé approximant to be sufficiently well constrained it was important to know the fermionic contribution to four loops. From the  $\beta$  function (13), and (6), we may now compute the running coupling  $\alpha_{qq}^{N_f=2}(\mu)$ . The result is shown in Fig. 6. As expected, the running coupling freezes at  $\alpha_{qq}^{N_f=2} \approx 0.5$  as  $\mu$  is taken to zero, rendering the theory scale invariant.

The question arises how reliable is our prediction of an infrared fixed point. Our main result is that at larger couplings the full, pure gauge  $\beta$  function is significantly smaller (in absolute terms) than its four-loop counterpart. That gives the fermionic part considerably more weight. In Fig. 7 we show the sum (12) of gluonic and fermionic contribution, in dependence on the number of loops of the fermionic part. Already at three loops the  $\beta$  function shows a second zero, which moves to  $\alpha_{qq}^{N_f=2} \approx 0.7$  at four loops and down to  $\alpha_{qq}^{N_f=2} \approx 0.5$  in case of the Padé approximant (13). This

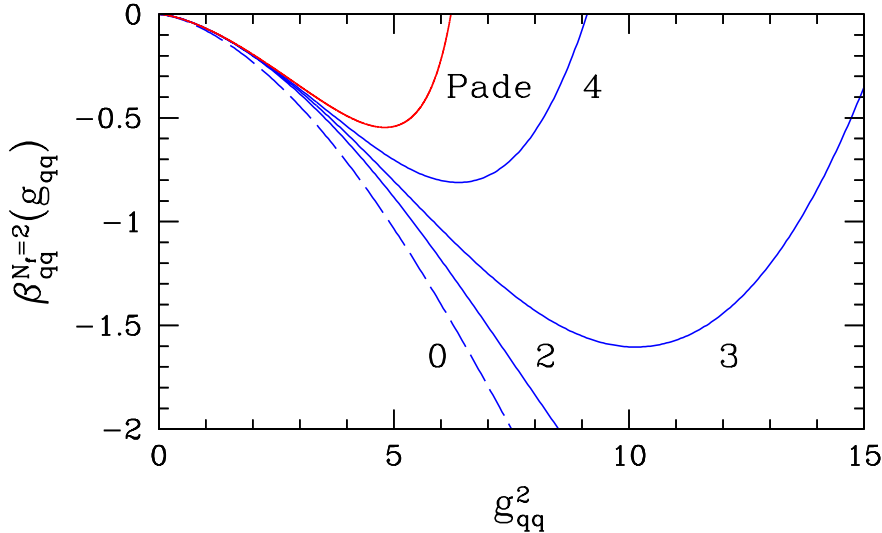


Figure 7: The pure gauge  $\beta$  function (11) plus the fermionic contribution to 0, 2, 3 and 4 loops, together with the Padé approximant of Fig. 5.



votes for the existence of an infrared fixed point for two massless quark flavors. The exact position of the second zero is subject to change though.

To conclude, we have shown that the pure gauge  $\beta$  function can be obtained from Wilson loops computed to very high order in numerical stochastic perturbation theory. First results from the  $12^4$  lattice are encouraging. The main source of uncertainty are discretization errors and, possibly, finite size corrections. We hope to extend the calculations to larger lattices in due course. This will allow us to probe the  $\beta$  function at even larger values of the coupling  $g_{qq}^2(L)$ . To corroborate our results on the infrared fixed point of the QCD  $\beta$  function for a small number of massless quarks beyond any doubts, we would need to compute the fermionic contribution to higher loops. That appears to be feasible. In [9] numerical stochastic perturbation theory has been extended to full QCD, and first results on Wilson loops have been reported. Perhaps, this is the only possibility of computing the  $\beta$  function for massless quarks at small virtualities.

## Acknowledgement

This work has been supported in part by the EU under contract 283286 (HadronPhysics3) and DFG under contract SCHI 422/9-1, which we gratefully acknowledge.

## References

- [1] I. I. Kogan and M. A. Shifman, Phys. Rev. Lett. **75**, 2085 (1995) [hep-th/9504141].
- [2] M. Lüscher, Nucl. Phys. B **180**, 317 (1981).
- [3] M. Donnellan, F. Knechtli, B. Leder and R. Sommer, Nucl. Phys. B **849**, 45 (2011) [arXiv:1012.3037 [hep-lat]].
- [4] R. Horsley, G. Hotzel, E.-M. Ilgenfritz, R. Millo, H. Perlt, P. E. L. Rakow, Y. Nakamura, G. Schierholz and A. Schiller, Phys. Rev. D **86**, 054502 (2012) [arXiv:1205.1659 [hep-lat]].
- [5] R. Alfieri, F. Di Renzo, E. Onofri and L. Scorzato, Nucl. Phys. B **578**, 383 (2000) [hep-lat/0002018].
- [6] F. A. Chishtie, V. Elias, V. A. Miransky and T. G. Steele, Int. J. Mod. Phys. A **16S1C**, 913 (2001) [hep-ph/0010053].
- [7] M. Göckeler, R. Horsley, A. C. Irving, D. Pleiter, P. E. L. Rakow, G. Schierholz and H. Stüben, Phys. Rev. D **73**, 014513 (2006) [hep-ph/0502212].

- [8] J. R. Ellis, I. Jack, D. R. T. Jones, M. Karliner and M. A. Samuel, Phys. Rev. D **57**, 2665 (1998) [hep-ph/9710302].
- [9] F. Di Renzo and L. Scorzato, JHEP **0410**, 073 (2004) [hep-lat/0410010].